GEOTECHNICAL AND GEOLOGIC CONSTRAINTS ON TSUNAMIGENIC SUBMARINE LANDSLIDES

H.J. LEE
U.S. Geological Survey, 345 Middlefield Road, Menlo Park, CA 94025 USA

Abstract

Modeling submarine-landslide-induced tsunamis requires many simplifications of the landslide process, although the real world is much more complicated. Clearly tsunami modelers cannot consider all facets, but there is value in being aware of the complications. This paper describes the many environments in which submarine landslides can occur and the triggers that typically initiate them. Earthquakes acting on continental or canyon slopes comprise probably the most common scenario but many other combinations of environments and triggers are possible. Surprisingly, many sediment-covered slopes in highly seismically active areas have not failed. A possible explanation for this phenomenon is a process called "seismic strengthening." The existence of such a process reduces somewhat the risk of landslide tsunamis along active margins while maintaining the risk along passive margins. Once a trigger has initiated a landslide in one of the vulnerable environments, failed masses begin to move downslope. Depending upon initial density state, the masses may convert into fluid-like sediment flows or even more dilute turbidity currents. A model for quantifying the tendency to flow is provided. Finally, a case study of the landslides and landslide tsunamis that occurred in Port Valdez, Alaska, during the 1964 Great Alaska Earthquake is provided. The excellent data base, including before and after bathymetry, shows that both large rigid block motion and mobilized sediment flows can occur near each other during the same event. The intact blocks are more efficient in producing tsunamis but the sediment flow can move farther and can erode and entrain considerable bottom sediment as they progress across the seafloor.

1 Introduction

Numerical modeling of submarine landslide initiation, motion and deformation, and the tsunamis that such physical processes produce, typically requires a great deal of simplification. Shapes of, and internal deformation within, failing landslide blocks must be idealized, failure triggers are often ignored, the risk of recurrence of events at a particular location are not considered. Clearly, all of the complications inherent in tsunamigenic submarine landslides cannot be modeled, but there is value in recognizing these factors so that the modeler can consider, at least qualitatively, what their impact might be in comparison with the factors that are being modeled.

This paper considers the following complicating factors that may play a role in the development of tsunamigenic submarine landslides and might be of interest to landslide tsunami modelers as they attempt to simplify the processes that are being modeled:

• Landslide environments
• Landslide triggers
• Influence of seismic loading history on sediment properties and landslide occurrence
• Landslide mobilization and morphology
• Influence of localized conditions on how landslides are generated and how they generate tsunamis

2 LANDSLIDE ENVIRONMENTS

Submarine landslides are not distributed uniformly over the world's oceans, but instead, they tend to occur most often where there are thick bodies of soft sediment, where the slopes are steep, and where the loads exerted by the environment are high. These conditions are met in fjords, deltas, submarine canyons, and on the continental slope (Lee et al., 2007a).

2.1 Fjords

Fjords with high sediment accumulation rates are one of the environments most susceptible to failure, both in terms of the proportional areal extent of deposits that can become involved in mass movement and also in terms of the recurrence interval of slope failures at a given location. Fjords are glacially eroded steep-walled valleys that have been inundated by the sea and are typically fed by sediment-laden rivers and streams that drain glaciers. These factors lead to conditions that are highly conducive to slope failure. For example, there is typically a delta at the head of the fjord, formed by streams draining the remnant of the glacier that initially eroded the valley with beds that dip at 5° to 30° between 10 and 50 m water depth, becoming less steep with water depth (Syvitski et al., 1987). The glacial streams feeding these deltas carry both rock flour and coarse sediment, whose deposits easily lose strength when shaken by an earthquake. Some fjord-delta deposits are so near instability that they fail during greater than average low tides, during which the supporting forces of the fjord waters themselves are temporarily removed from the sediment.

In addition to the fjord-delta deposits, the sidewall slopes of fjords also can be unstable. Deposition of suspended sediment on the steep (10° to 90° overhangs) submerged valley sides can frequently lead to small slope failures (Farrow et al., 1983). Even more important are slope failures on side-entry deltas that build out rapidly onto the sidewall slopes (Terzaghi, 1956; Prior et al., 1981).

Because fjords are commonly found in rugged mountainous terrain, the unstable fjord-head deltas and side-entry deltas are frequently the only flat land available for coastal development. Not only do these developments become vulnerable to natural slope failure, but human activities also can lead to additional slope failures.

2.2 Active river deltas on the continental shelf

Within active deltas, rivers rapidly contribute large quantities of sediment to relatively localized areas. Depending upon such environmental factors as rate of sediment influx, wave and current activity, and the configuration of the continental shelf and coastline, thick deltaic deposits can accumulate fairly rapidly and can become the locations of sediment instability. Large deep-seated landslides can result when a thick deposit containing comparatively low-strength sediment or weak zones occurs. In addition, decaying organic matter can produce bubble-phase gas that can further reduce strength. These locations may fail under gravitational loading (due to the slope steepness alone) or during storms or earthquakes.

Locations of major sedimentary depocenters that have produced large landslides include glacially fed rivers delivering rock flour onto high latitude shelves (Schwab and Lee, 1983), and temperate rivers such as the Mississippi (Coleman et al., 1980) and the Huanghe (Prior et al., 1986).

2.3 Submarine canyon-fan systems

Submarine canyon-fan systems serve as conduits for passing large amounts of sediment from the continental shelf to the deep sea. The presence of extensive, thick sediment fans and abyssal plains off the coasts of many areas testifies to the importance of mass-movement mechanisms associated with these systems. Landsliding, particularly within submarine canyons, appears to be an important, if not essential, part of the process (Hampton, 1972). However, the circumstances surrounding these slope failures (including their initial size) and their subsequent conversion into debris flows and turbidity currents are poorly understood. These processes were likely more common during glacial cycles (Nelson, 1976; Barnard, 1978) than they are today.

2.4 The open continental slope

A final common environment for undersea landsliding is the intercanyon area of the continental slope far removed from submarine canyon-fan systems and river deltas. An example of a significant open slope landslide is the Storegga Slide off Norway, with a runout distance of 810 km and a volume of 2400 to 3200 km^3. At Storegga, contrasting sedimentation conditions produced clay layers with excess pore pressures during interglacials, overlain by glaciomarine layers during glacial cycles. Owing to rapid sedimentation, some of these layers contain excess pore pressures. The resulting weak layers provide a plane along which failure can occur, although the failures are still likely triggered by earthquakes (Bryn et al., 2003; Canals, 2004). Large failures have occurred at the site of the Storegga Slide at semi-regular intervals over the last 500 ky, with the most recent large failure occurring 8200 years ago. The Storegga example shows that complex environmental and sedimentological conditions lead to ultimate failure at a particular location and that large failures can occur at the same location over and over again throughout geologic time.

Open-continental-slope failures are found near river mouths and far removed from them, as well as in both arid and humid climates. Ages of the slope failures are seldom known

(the Storegga Slide is one of the few exceptions), so investigators cannot determine whether they occurred under glacial or interglacial conditions. Many were probably seismically induced because the typical gradients of continental slopes are 5° or less and the seabed should be statically stable (unless very weak layers are present), and because storm-wave loading is seldom a major factor much below the shelf break (Lee and Edwards, 1986). Some failures appear to be related to the presence of relatively weak sediment layers.

3 LANDSLIDE TRIGGERS

Submarine landslides are triggered either by an increase in the downslope driving stresses, a decrease in strength, or a combination of the two (Lee et al., 2007a). The following possible triggers show the interplay of these factors. Note that the relative importance of each of these triggers is not well understood. In some environments one of these triggers will dominate, whereas in others a different trigger will be most significant.

3.1 Sediment accumulation

Rapid sediment accumulation can contribute to slope failure. When sediment accumulates rapidly, much of the weight of newly added sediment is carried by pore-water pressures and does not increase the resisting shear strength significantly. However, the shear stress acting downslope increases rapidly with the weight of new sediment deposited. Also, the slope may steepen because more sediment accumulates at the top of the slope. As a result, the factor of safety of the slope decreases. The Mississippi Delta is an ideal example of sediment failure induced by sediment accumulation. (Prior and Coleman, 1978)

3.2 Erosion

Localized erosion by moving water or sediment flows, is common in deep-sea channels, submarine canyons and other active sediment-transport systems. When seabed surfaces are undercut, this can decrease the stability by increasing shear stress and in some cases decreasing the shear strength. Monterey Canyon, located off central California, shows many examples of erosion-induced slope failures. Often, these failures dam the canyon so that subsequent turbidity-current flows are diverted, leading to further erosion and second-generation landslides (Greene et al., 2002).

3.3 Earthquakes

Earthquakes are called upon as a cause for many unexplained submarine landslide features (e.g. Hampton et al., 1996, Lee and Edwards, 1986). One reason is that earthquake-induced shear stresses do not result in corresponding increases in shear strength and accordingly reduce the slope factor of safety. A second reason in that earthquakes generate excess pore water pressures through cyclic loading, which can lower the strength, possibly induce a state of liquefaction, and reduce the factor of safety even more. Examples of earthquake-induced submarine failures are numerous and

include the 1929 Grand Banks event (Piper et al., 1999), multiple failures in Alaskan Fjords during the 1964 earthquake (Coulter and Migliaccio, 1966) and the 1998 Papua New Guinea earthquake and tsunami (Tappin et al., 2003).

3.4 Volcanoes

Giant submarine landslides have been mapped all around the flanks of the Hawaiian Islands (Moore et al., 1989, Normark et al., 1993). Further work (Holcombe and Searle, 1991) has shown that the Hawaiian Islands are not alone, and that many, if not most, oceanic volcanoes fail catastrophically during part of their existence. Some component of oceanic volcanism is clearly a trigger for submarine landslides, but the nature of that component has not been determined. Most of the larger, older landslides seem to have occurred late in the shield-building phase of the host volcano (Moore et al., 1989).

3.5 Waves

That storm-waves can trigger slope failure was illustrated by damage to offshore drilling rigs during Hurricane Camille in 1969 (Bea et al., 1983). Storm-wave-induced failure can occur as the passage of a wave train subjects the seafloor to alternating water pressure as the crests and troughs pass (Henkel, 1970, Seed and Rahman, 1978). This non-uniform pressure field induces shear stresses between crest and trough. These shear stresses are much like earthquake loads in that they add to preexisting downslope gravitational stresses and they are cyclic in nature, so that they gradually cause pore-water pressures to increase in the sediment. The sediment can fail after the passage of a wave train, or it can liquefy and flow if the pore pressures reach a high enough value (Van Kessel and Kranenburg, 1998).

3.6 Gas and gas hydrates

Gas charging of sediment itself is not so much a trigger as a means by which shear strength may be altered. Gas charging decreases sediment strength through the development of excess pore pressures. If strength is reduced enough, another trigger, such as an earthquake, can cause actual failure.

Dissociation of gas hydrates has been suggested as a mechanism for reducing shear strength at the base of a gas hydrate zone (Kayen and Lee, 1991). The process would often be most effective during periods of sea level lowering or water column warming. Sultan et al. (2003) modeled the impact of sea-level rise and warming of the North Atlantic on the stability of the Norwegian continental slope where the giant Storegga Slide occurred (Bryn et al., 2003). Sultan et al. (2003) suggested that increases in pressure and temperature associated with the end of the last glacial period could have induced a dissociation of methane hydrate at the top of the hydrate layer, leading to massive slope failure. Such a mechanism for producing the Storegga slide is still being debated.

3.7 Groundwater seepage

Many investigators have suggested that the flow of fluids through submarine sediment bodies can lead to slope failures. For example, Sangrey (1977) speculated that underconsolidation and excess pore pressures resulting from artesian reservoir sources are "very common offshore and may be the most significant mechanism" for causing slope failure. In addition, Orange and Breen (1992) suggested that pore fluids percolating up from subducted sediment could induce slope failure and lead to the development of headless canyons, i.e., submarine canyons that are not linked to incised valleys on the shelf. Robb (1984) suggested that spring sapping (i.e., erosion of sediment and rock by underwater springs) may have occurred on the lower continental slope off New Jersey during periods of lowered sea level.

As another undersea-groundwater-seepage mechanism for causing nearshore failures, investigators have pointed to a phenomenon that engineers term rapid drawdown (Lambe and Whitman, 1969, p. 477). This process is illustrated by failures that often occur in fjords and other coastal locations during periods of low tides (e.g., Prior et al., 1982a, 1982b). During low tides, water levels fall rapidly, and pore pressures within coastal slopes often cannot adjust quickly enough. This results in an elevated water table directly adjacent to the coast and in accelerated seepage of ground water. This situation can be modeled as seepage forces, that effectively add downslope driving stress, or as excess pore pressures, that reduce the effective stress and the corresponding sediment shear strength. Liquefaction in the Fraser delta has been modeled by considering tidal variations that cause unequal pore-pressure generation (Atigh and Byrne, 2004)

3.8 Diapirism

Any tectonic or diapiric deformation that results in steepened seabed surfaces will lead to a reduction in the factor of safety and increased likelihood of slope failure. The northern Gulf of Mexico is an area in which diapiric deformation is one of the major causes of failure on the continental slope. Martin and Bouma (1982) noted that masses of Jurassic salt and Tertiary shale underlie the northern Gulf of Mexico continental slope and adjacent outer continental shelf. Large overburden pressures created by sediment accumulation from the late Jurassic to the present have caused the underlying salt and shale sheets to flow and sometimes extrude toward the surface. These movements are largely responsible for the surface morphology (Silva et al., 2004), which in turn has produced numerous slope failures.

3.9 Human activity

Human-constructed facilities, either along the coastline or on the seafloor have the potential for causing submarine slope failures by increasing downslope stresses in the sediment column. An example of such a failure occurred in Rissa, Norway in 1978 (Gregersen, 1981), in which the placement of earth fill near the shore of a lake caused the development of a "quick clay river" that transported buildings and farms into the lake.

Another event occurred in Nice, France, in 1979, and involved a failure of fill that had been placed near a delta to construct a new airport (Seed et al., 1988). The slide occurred over a period of about four minutes and involved debris moving down the sloping face of the delta deposit, into a submarine canyon, and onto an abyssal plain. A tsunami struck the coastline with a maximum amplitude of 3 m, taking several lives. A similar case occurred in Skagway Alaska in 1994, when a dock that was under construction slid into a fjord. A particularly low tide was accompanied by a series of tsunami waves estimated to be as high as 11 m (Rabinovich et al., 1999) and one life was lost. Finally, in 1985, near Duwamish Head in Seattle, Washington (Kraft et al., 1992), dredging operations were undertaken to extend sewage effluent pipes offshore. During low tide, a landslide occurred around the site of the dredging operations. The landslide was clearly triggered by the low tide, but the dredging operation was an underlying cause.

4 INFLUENCE OF SEISMIC LOADING HISTORY ON SEDIMENT PROPERTIES AND LANDSLIDE OCCURRENCE

As discussed previously, earthquakes are often considered to be a particularly important trigger for submarine slope failure. However, as will be seen below, many continental slopes in highly seismically active areas have not failed whereas slope failures in less seismically active areas actually seem to be more prevalent. Lee et al. (2004) speculated that one factor that may contribute to the relatively low occurrence of slope failures in some seismically active environments is sediment response to cyclic loading history. That is, sedimentary bodies that are exposed to a long history of seismic loading from small to moderate earthquakes may strengthen themselves as a result of this history and become better suited for withstanding future earthquake shocks.

4.1 The prevalence of continental slope failures

McAdoo et al. (2000) evaluated acoustic imagery from large sections of the U.S. continental slope using Geographic Information System (GIS) software and identified a total of 83 mass movement deposits. The authors considered four distinctly different tectonic environments on the continental slopes of Oregon, central California, Texas, and New Jersey. The analysis showed that the slope in the Gulf of Mexico has the highest percentage (27%) of its surface area covered with failures. The next highest percentage is for New Jersey (9.5%), followed by California (7.1%) and Oregon (3%). Interestingly there is a rough inverse relation between the area covered by landslides with the seismicity.

Within smaller sections of the highly active California margin, several areas have been mapped in detail using multibeam bathymetric mapping techniques (Locat et al., 1999). In Santa Barbara Channel, several large and a number of smaller slope failures are apparent (Fig. 1, Eichhubl et al., 2002). At least one of the smaller failures may only be a few hundred years old but the large failure near the center of the image is about 5000 years old (Lee et al., 2004). Other ancient failures have occurred at the location of the large failures as recorded in subbottom profiles and likely have a recurrence interval of about 15,000 years (Lee et al., 2004). Unfailed smooth slopes, lying to the west of the

major failures (for example in the area of core 601 P1), have apparently been stable for long periods of geologic time, certainly in the range of thousands of years. Again, during this period of stability, hundreds of large earthquakes must have occurred without causing the slope to fail.

Fig. 2, which shows multibeam imagery from a section of the southern California margin off the coast of the City of Los Angeles, also shows the distribution of landslides. One part of this image from the continental slope off the Palos Verdes Peninsula shows multiple shallow- and deep-seated slope failures. However, most sections of the slope are smooth, sedimented and apparently unfailed.

These two figures show several dramatic slope failures but a general paucity of landslides in one of the most seismically active margins of the United States. These figures support the general findings of McAdoo et al. (2000) that the west coast of the United States has a relatively lower concentration of continental slope submarine landslides than do other U.S. continental margins.

4.2 Analysis

Lee and Edwards (1986) used a modified form of Morgenstern's (1967) infinite slope analysis for seismic loading of submarine slope. Earthquake loads are represented by a pseudo-static acceleration. For a factor of safety of 1, the critical pseudo-static earthquake acceleration, k_c, is:

$$k_c = (\gamma'/\gamma) [S (OCR)^m - \sin \alpha] \qquad (1)$$

where (γ'/γ) is the ratio of buoyant to total density (typically about 1/3), S is the ratio of undrained shear strength to overburden effective stress for normal consolidation (typically about 0.3), OCR is the overconsolidation ratio, m is a constant (typically = 0.8) derived from a normalized soil parameter approach (Ladd and Foott 1974) and α is the slope steepness. Accordingly, for typical values, normal consolidation (OCR = 1), and no slope, the critical acceleration is 0.1 *g*. For a typical slope of around 4°, k_c becomes 0.076 *g*. Such low values of acceleration would likely be exceeded frequently along the coast of California. Only with some level of OCR can higher critical accelerations be obtained, allowing submarine slopes to withstand repeated seismic shaking.

4.3 The impact of seismic shaking

We generally think of seismic shaking as contributing to a reduction in sediment shear strength. In fact, in the case of loose, cohesionless soils, we know that seismic shaking can lead to liquefaction, loss of bearing capacity, and collapse of engineering structures. For cohesive sediment we have found that there is also a loss in shear strength with a single burst of cyclic loading. For example, based on an extensive series of cyclic triaxial tests on sediment from off the coast of sourthern Alaska, we found that the cyclic strength (defined as cyclic stress level necessary to cause 20% axial strain in 10 cycles) ranged

between 40% and 105% of static strength, depending upon plasticity (Lee and Edwards, 1986).

One of the reasons that cyclic loading causes a reduction in shear strength, or even liquefaction, is that cyclic loads transfer overburden stress from interparticle contacts to the interstitial water. This transfer causes an increase in pore water pressure and a decrease in effective stress. Such changes cause an immediate decrease in strength.

If the sediment column can survive an earthquake and not fail, some of the excess pore water pressures generated by seismic shaking will remain and slowly dissipate with time. Such dissipation will result from pore water drainage out of the sediment fabric and will correspond to sediment densification. This densification can result in apparent overconsolidation, a net gain in undrained shear strength and an enhanced ability of the sediment fabric to resist cyclic loads in the future. One would expect that future earthquakes would have a similar effect, although perhaps with decreasing amounts of densification and strength gain.

4.3 Field evidence

A piston core sample was obtained in the Santa Barbara Channel of southern California on an apparently stable slope between the remains of two large slope failure deposits (Figure 1, Core 601P1). Several of the core sections were split and fall cone penetrometer tests were conducted downcore to determine the undrained shear strength profile. Figure 3 shows these results as well as an estimate of what the strength profile would be if the sediment were normally consolidated (S assumed equal to 0.3). As may be seen the measured shear strengths exceed the normally consolidated values by a factor of 2 or more, indicating a significant level of apparent overconsoldiation. As an indication of age control and seismicity, the accumulation rate in this region is about 1 mm/yr (Lee et al., 2004) and the last major earthquake in this area occurred in 1812 (corresponding to a depth in core of about 20 cm). If large earthquakes occur every few hundred years, then the 5 m long sequence shown by Core 601P1 represents perhaps 20 large earthquakes.

4.4 Laboratory simulations

Laboratory simulations of seismic strengthening were conducted at Laval University (Boulanger et al., 1998, Boulanger, 2000). In these simulations, sediment samples were consolidated to a predetermined vertical consolidation stress level, σ_{vc}'. Next the samples were subjected a set of shear stress cycles and the amount of pore pressure development was measured. Pore water was allowed to flow out of the sample and the generated excess pore water pressures were allowed to dissipate. Additional bursts of cyclic loading were then applied, followed by a period of pore water drainage. The overall response of the cyclically loaded sediment sample was compared with the response of a sample that was not cyclically loaded. From this comparison, the degree of induced overconsolidation could be determined. Also, both the seismically-strengthened

sample and the normally loaded sample were failed after the simulation to determine their shear strengths.

Fig. 4 shows the results of such a simulation. One reconstituted sediment sample was consolidated normally to progressively higher vertical stress levels. A second, identical sample was consolidated to a particular vertical effective stress level and then subjected to four bursts of undrained cyclic loading, with pore water drainage allowed after each burst. Figure 4 shows that each cyclic burst/reconsolidation cycle caused densification (reduction in void ratio) of the sample, although the amount of densification became smaller with each burst. Likewise, the amount of pore pressure generated also decreased with each burst. Fig. 4 shows that the bursts of cyclic loading produced greater densities (lower void ratios) than would be expected for normal consolidation, in effect showing that the cyclically loaded sample became progressively more overconsolidated with each cyclic loading/subsequent drainage episode. Using conventional geotechnical techniques (Casagrande, 1936) the overconsolidation ratio (OCR) was obtained for the sediment after each cyclic burst. An estimate of static shear strength, s_u, was then obtained using normalized soil parameters (Ladd and Foott, 1974; Lee and Edwards, 1986) with S = 0.3 and m = 0.8 as discussed previously:

$$s_u = S\ OCR^m \qquad (2)$$

For this particular test, the estimated shear strength was found to increase by 67% after only 3 "earthquakes."

4.5 Summary of findings regarding seismic strengthening

The morphology of slopes in seismically active areas shows fewer landslides than one might expect given the apparent severity of loading that earthquakes produce on the seafloor. A comparison of continental slopes around the margins of the United States shows an almost inverse relation between landslide occurrence and seismicity. Within study areas off the coast of California, where highly accurate bathymetry has been obtained, a few large landslide deposits are observed but a majority of sedimented slopes have not failed.

Within an area of unfailed slope between two large slope failures in Santa Barbara Channel, the sediment shear strength was found to be at least twice as large as would be expected for normally consolidated sediment. A possible explanation for this observation is that the sediment is unusually strong because of the process of "seismic strengthening." With each passing earthquake the sediment excess pore pressure is increased. If the sediment does not fail immediately, the excess pressures dissipate through pore water drainage out of the deposit. Accordingly, the sediment may become strong enough to withstand most future earthquakes. Laboratory simulations show that the process of seismic strengthening is effective and leads to significant strength gains.

5 LANDSLIDE MOBILIZATION INTO SEDIMENT FLOWS

Following initial failure, some landslides mobilize into flows whereas others remain as limited deformation slides (Hampton *et al*. 1996). The mechanisms for mobilization into flows are not well understood but the initial density state of the sediment is likely to be one important factor (Poulos *et al*. 1985, Lee *et al*. 1991). If the sediment is initially less dense than an appropriate steady-state condition (contractive sediment) the sediment is more likely to flow than one that is denser than the steady-state condition (dilatant sediment) (Fig. 5). The steady state represents a boundary between contractive and dilatant behavior and is described by the porosity-effective stress conditions that a sediment will assume when strained by a large amount. This response is an example of how pore pressures are generated during failure; contractive sediment generates positive pore pressure during shear and these increased pore pressures reduce the strength. Contractive failure of loose sedimentary deposits can occur at constant porosity. The sediment essentially collapses upon itself and loses much of its strength in the process. Dilatant sediment generates negative pore-water pressures during shear and becomes stronger in the process. The ability to flow also may be related to the amount of energy transferred to the failing sediment during the failure event (Leroueil *et al.,* 1996, Locat and Lee, 2002).

Strength loss at constant porosity cannot explain the behavior of some far-reaching debris flows (Schwab et al., 1996; Locat et al., 1996). For example, there is evidence for debris flows reaching the distal lobes of the Mississippi Fan that must have flowed for roughly 500 km on slopes as gentle as 0.06° (Locat et al., 1996). If these deposits represent such flows, then an estimate for the threshold yield strength is 9 Pa. Such a low value is 3 orders of magnitude lower than an estimated remolded shear strength in the presumed source region (Locat et al., 1996). Accordingly, the sediment must have taken on additional water during flow, increasing its porosity and decreasing its strength, or the flow must have hydroplaned. The dilution mechanism is consistent with that suggested by Hampton (1972), who described an increase in the sediment water content caused by the jostling and deformation within the sediment during the remolding phase of the failure event. This greatly reduces the shear strength and provides a fluid-like behavior to the mixture. During this dilution process, however, the water content cannot become so high that the resulting flow transforms into a turbidity current. In the example of the Mississippi Fan debris-flow deposits, the presence of clasts demonstrates that the sediment flow still retained competence and was not so energetic as to cause the clasts to disintegrate.

6 INFLUENCE OF LOCALIZED CONDITIONS ON HOW TSUNAMIGENICE LANDSLIDES ARE GENERATED AND TRANSFORMED (CASE STUDY, PORT VALDEZ, ALASKA)

6.1 Introduction

A problem with underwater, tsunamigenic landslides is that they typically cannot be observed directly. Rather, the effects of the landslide are generally seen, but the causes of the effects must be inferred. There are a number of good case studies that have been used

to advance the field but one of the best is the response of the seafloor and water column in Port Valdez, Alaska, to the Great Alaska Earthquake of 1964 (Mw = 9.2).

The event was the largest earthquake ever recorded in North America, and there was major damage to all of the coastal communities in south-central Alaska. Valdez, a small town on the shores of the glacial fjord known as Port Valdez was particularly hard hit (Coulter and Migliaccio, 1966). A total of 32 people died in Valdez, most as the result of tsunamis with runups of up to 50m that were induced by submarine landslides that also destroyed the waterfront (Parsons et al., 2014). Following the earthquake, extensive investigations were conducted of the effects of the earthquake on Alaska's communities and landscape (Coulter and Migliaccio, 1966; Plafker et al, 1969). These studies showed dramatic changes in bathymetry off the fjord-head delta near the town of Valdez (up to 100 m of deepening) and the highest tsunami wave runup heights measured anywhere in Alaska during the event. Tsunami waves at the waterfront of Valdez were estimated to have been 10-12 m (Coulter and Migliaccio, 1966), but the greatest tsunami wave runup heights (52 m, Fig. 6) were in the western part of the fjord, at the opposite end from the community (Plafker et al., 1969). Recent multibeam maps of the fjord and new high-resolution subbottom profiles, coupled with a reassessment of pre- and post-earthquake bathymetry have expanded the available database.

Preliminary findings from these data sources (Lee et al., 2006, Ryan et al., 2009) note the presence of several large blocks (40-m high and 300-m across) on the basin floor near a moraine deposit in the western part of the fjord (front of Shoup Bay, Fig. 6) and a complex series of gullies and chutes in the area off the old community where depth increased by over 100 m during the earthquake. The large blocks resulted from a failure of the moraine front during the earthquake and their motion likely contributed to the particularly high waves observed immediately onshore from them. The bathymetric map also shows a subtle north-south trending step near the middle of the fjord, which appears to be the front of a large debris lobe that flowed westward from the fjord-head delta (Fig. 6). In general, these results show that radically different landslide morphologies can result from the same event. Also, they illustrate that Port Valdez acts as a natural flume, within which landslides are generated at one end, transform into debris flows, and proceed downslope and along the basin flow more or less as a two-dimensional event.

6.2 Results

6.2.1 Sediment volumes based on bathymetric changes, 1901-1966

Two hydrographic surveys conducted by the U. S. Coast and Geodetic Survey in 1901 and 1966 were available for Port Valdez, spanning the 1964 earthquake. Differences in bathymetry between 1901 and 1966 show areas as much as 40 m shoaler southeast of Shoup Bay and as much as 60 m deeper near the fjord head. Overall, the bathymetric difference map (Fig. 7, Lee et al., 2006. Ryan et al., 2009) shows a shoaling over 60% of the surface area, with a deepening over 40% of the fjord. Volumetric calculations show 4.3×10^8 m^3 removed from the area that deepened near the fjord head and an increase in volume of 3.8×10^8 m^3 over the fjord floor area that shoaled.

Accordingly, the sediment budget roughly balances and shows significantly more sediment movement than reported by previous investigators for a localized area near the fjord head (75 x 10^6 m^3, Coulter and Migliaccio, 1966).

6.2.2 Sediment volume based on acoustic stratigraphy

A longitudinal subbottom profile (Fig. 8) illustrates the overall landslide and sediment stratigraphy of Port Valdez. The deepest sedimentary unit is generally a finely layered sequence that appears to be typical fjord sedimentation, such as was occurring prior to the earthquake. Lying above the layered sequence in many locations is a chaotic to transparent facies, which appears to be debris flow material brought down by slope failures during the 1964 earthquake. An acoustic reflector (red line in Fig. 8) separates the layered (pre-1964) and chaotic (1964) facies over much of the fjord. The thickness of the debris flows (difference between water bottom and top of the layered unit) was determined and used to calculate the volume of material above the surface of layered sediment as $9.8x10^8$ m^3. At the eastern end of the fjord, the layered sediment was at or near the sea floor; at the middle to western end of the fjord, it was as much as 30-40 m beneath the sea floor.

6.3 Discussion

As noted above, the floor of the eastern 40% of Port Valdez deepened during the 1964 earthquake, including the fjord-head delta where massive failures were directly observed at the waterfront of old Valdez (Coulter and Migliaccio, 1966). However, the area of sediment removal also includes a low seafloor gradient (~2°) region west of the fjord-head delta. This appears to suggest that the seafloor did not fail directly in this section, but rather was scoured by erosive debris flows moving westward from the delta head.

As discussed above, by integrating the thickness of sediment lying above the surface of layered sediment (Fig. 8), the volume of landslide debris was calculated to be $9.8x10^8$ m^3 (nearly 1 km^3). This is in stark contrast to the value calculated from bathymetric differences over the area that shoaled ($3.8x10^8$ $m^{3)}$. That is, more than twice as much material is deposited as landslide debris than is represented by shoaling of the seafloor. These results suggest that the debris flows were very erosive when they entered a zone that would ultimately become depositional. The flows eroded some of this area, incorporated the sediment into the flow and essentially doubled the volume of flowing material. A similar phenomenon was observed in the tsunamigenic submarine debris flow at Kitimat, British Columbia in 1975, where more than half of the debris flow mass was derived from incorporated fjord-bottom sediment (Prior et al., 1984). The entire deposit was ultimately emplaced in the deep basin with a landslide debris thickness of as much as 30 m. Note in Fig. 8 that the landslide deposit is thickest toward the eastern part of the depositional zone and thins toward the west. This likely indicates that the ability of the flow to scour decreased as it moved westward, gradually leaving thinner deposits. Scouring by debris flows has also been reported from other marine settings (Canals et al., 2004; Lastras et al., 2004).

The debris flow that began at the fjord-head delta and moved west was clearly the most significant failure component produced in Port Valdez by the 1964 earthquake. However, there were also failures contained in the western part, including large blocks generated by the failure of the Shoup Bay moraine (Figs. 6 and 7). The blocks form two clusters, one to the southeast of the moraine (smooth, pointed promontory south of Shoup Bay itself) and one to the southwest. Behind (north of) each set of blocks is a zone of sediment removal shown by the bathymetric difference map (Fig. 7), likely indicating gouging or eroding of the seafloor as the blocks translated across the bottom. The highest tsunamis for the earthquake were recorded near this moraine failure (Fig. 6), indicating that intact blocks are more efficient tsunami generators than more deformed flows (Rabinovich et al., 2003).

7 CONCLUSIONS

This paper discussed some of the complexities of submarine landslides that must often be ignored by those modeling how such landslides generate tsunamis. These include assessing which parts of the world's ocean are more susceptible to failure than others, such as fjords, active deltas, submarine canyons and the open continental slope. Also, modelers often do not take into account what factors actually produce tsunamigenic submarine landslide. These can include sediment accumulation and erosion, earthquakes and storm waves, volcanic activity, groundwater seepage and gas charging. Each of these triggers is unique and can produce different forms of landslide behavior.

Earthquakes are commonly thought of as the most common trigger for submarine landslides and resulting tsunamis. However, a long series of moderate earthquakes at a particular location on the seafloor, if none is large enough to produce failure in itself, may be able to slowly strengthen the sediment and reduce the likelihood of failure. A result of this process can be that sediment failures in seismically active areas are less common than those in less seismically active areas.

Following initial failure of submarine slopes, the failing sediment body moves downslope and can convert from a rotating or sliding block into a fluid-like sediment flow, and possibly into a lower density turbidity current (Hampton, 1972). The ability of block slides to convert into sediment flows and turbidity currents seems to be related to the initial density state of the sediment, with relatively dense sediment bodies remaining as blocks and loose bodies converting rapidly into flows. Block slides seem to be more efficient generators of tsunamis.

Finally, Port Valdez, Alaska, is an excellent natural laboratory for studying submarine landslides and landslide-induced tsunamis. The 1964 Alaska Earthquake occurred after bathymetric surveys had been conducted in the fjord and a town had been built on its margin. Post-earthquake surveys showed how the geometry of the fjord floor had changed, the runup heights of tsunamis all around the fjord, and the overall landslide morphology of the floor. There were also numerous eyewitnesses to the tsunamis and coastline damage. The studies showed that the movement of rigid blocks in the western part of the fjord were the most efficient initiators of tsunamis, even though much larger

failures occurred in the eastern end but these quickly mobilized into sediment flows. Subbottom geophysical surveys appear to show that the sediment flows were very erosive and incorporated considerable bottom sediment into the moving mass of material dislodged from the fjord head.

REFERENCES

Atigh, I. and Byrne, P.M. (2004) Liquefaction flow of submarine slopes under partially undrained conditions: an effective stress approach. *Can. Geotech. J.,* **41**, 154-165.

Barnard, W. (1978) The Washington continental slope: Quaternary tectonics and sedimentation. *Mar.Geol*, **27**, 79-114.

Bea, R.G., Wright, S.G., Sircar, P., and **Niedoroda**, A.W. (1983) Wave-induced slides in South Pass Block 70, Mississippi Delta. *J. of Geotech. Eng.*, **109**, 619-644.

Boulanger, E. (2000) Comportement cyclique des sédiments de la marge continentale de la rivière Eel: une explication possible pour le peu de glissements sous-marins superficiels dans cette région. M. Sc. Thesis, Department of Geology and Geological Engineering, Laval University.

Boulanger, E., Konrad, J.-M., Locat, J., and Lee, H.J. (1998) Cyclic behavior of Eel River sediments: a possible explanation for the paucity of submarine landslide features. American Geophysical Union San Francisco, EOS, Abstract.

Bryn, P., Solheim, A., Berg, K., Lien, R., Forsberg, DC.F., Haflidason, H., Ottesen, D., and **Rise, L**. (2003) The Storegga slide complex: repeated large scale sliding in response to climatic cyclicity, In: *Submarine Mass Movements and their Consequences, 1st Inter. Symp.* (Eds. J. Locat and J. Mienert), Kluwer, 215-222.

Canals, M., Lastras, G., Urgeleas, R., *et al.* (2004) Slope failure dynamics and impacts from seafloor and shallow sub-seafloor geophysical data: case studies from the COSTA project. *Mar. Geol.*, **213**, 9-72.

Casagrande, A. (1936) The determination of the Pre-consolidation load and is practical significance, *Proc. 1st Int. Conf. Soil Mech. Found. Eng.* (Cambridge MA) 60.

Coleman, J.M., Prior, D.B., and **Garrison, L.E**. (1980) Subaqueous sediment instabilities in the offshore Mississippi River delta. *U.S. Bureau of Land Management Open-file Report,* **80-01**, 60.

Coulter, H.W. and **Migliaccio, R.R**. (1966) Effects of the earthquake of March 27, 1964 at Valdez, Alaska. U.*S. Geol. Survey Professional Paper*, **542-C**.

Eichhubl, P., Greene, H.G. and N. Maher, N. (2002) Physiography of an active transpressive margin basin; high-resolution bathymetry of the Santa Barbara Basin, southern California continental borderland. *Mar*. *Geol*., **184**, 95–120.

Farrow, G.E., Syvitski, J.P.M., and **Tunnicliffe, V**. (1983) Suspended particulate loading on the macrobenthos in a highly turbid fjord: Knight Inlet, British Columbia. *Can. J. of Fisheries and Aquatic Sci.*, **40(suppl. 1)**, 273-288.

Gregersen, O. (1981) The quick clay landslide in Rissa, Norway. *Proc., 10th Int. Conf. On Soil Mech. and Found. Eng*., **3**, 421-426.

Greene, H.G., Maher, N.M., and **Paull, C.K**. (2002) Physiography of the Monterey Bay national Marine Sanctuary and implications about continental margin development. *Mar. Geol.*, **181**, 55-82.

Hampton, M. (1972) The role of subaqueous debris flow in generating turbidity currents.

Jour. of Sed. Petr., **42**, 775-993.
Hampton, M., A., Lee, H.J., and **Locat, J.** (1996) Submarine landslides. *Rev. of Geophys.*, **34**, 33-59.
Henkel, D.J. (1970) The role of waves causing submarine landslides. *Geotechnique*, **20**, 75-80.
Holcomb, R.T., and **Searle, R.C.** (1991) Large landslides from oceanic volcanoes. *Mar. Geotech.*, **10**, 19-32.
Kayen, R.E. and **Lee, H.J.** (1991) Pleistocene slope instability of gas hydrate-laden sediment on the beaufort sea margin. *Mar. Geotech.*, **10**, 125-141.
Kraft, L.M., Gavin, T.M., and **Bruton, J.C.** (1992) Submarine flow slide in Puget Sound. *J. of Geotech. Eng.*, ASCE, **118**, 1577-1591.
Ladd, C. C. and Foott, R. (1974) New design procedure for stability of soft clays, *J. Geotech Eng. Div., ASCE,* **100**, 763-786.
Lambe, T.W. and **Whitman, R.V.** (1969) *Soil Mechanics*, John Wiley, New York, 553 pp.
Lastras, G., Canals, M., Urgeles, R., De Batist, M., Calafat, A.M. and Casamor, J.L. (2004) Characterisation of the recent BIG'95 debris flow deposit on the Ebro margin, Western Mediterranean Sea, after a variety of seismic reflection data. *Mar. Geol.*, **213** (1-4), 235-255.
Lee, H.J. and **Edwards, B.D.** (1986) Regional method to assess offshore slope stability. *Jour. of Geotech. Eng.*, ASCE, **112**, 489-509.
Lee, H.J., Normark, W. R. Fisher, M. A.; Greene, H. Gary, Edwards, B. D., and Locat, J., (2004) Timing and extent of submarine landslides in southern California, *Offshore Tech Conf.* #16744, Houston, TX.
Lee, H.J., Orzech, K., Locat, J., Konrad, J.-M., and Boulanger, E. (2004) Seismic strengthening, a conditioning factor influencing submarine landslide development, *Proc., 57th Can. Geotech. Conf.,* 7 pp.
Lee, H.J., Locat, J., Dartnell, P., Minasian, D., and Wong, F. (2000) A GIS-based regional analysis of the potential for shallow-seated submarine slope failure, *Proc., 8th Int. Symp. on Landslides*, 917-922.
Lee, H.J., Locat, J., Desgagnes, P., Parsons, J.D., McAdoo, B.G., Orange, D. L., Puig, P., Wong, F.L., Dartnell, P., and Boulanger, E. (2007a) Submarine Mass Movements on Continental Margins, in: Nittrouer, C.A., Austin, J.A., Field, M.E., Kravitz, J.H., Syvitski, J.P.M., and Wiberg, P.L., eds., Continental-Margin Sedimentation: from Sediment Transport to Sequence Stratigraphy, IAS special publication 37, Chapter, 213-274, Blackwell Publishing Ltd., Oxford.
Lee, H., Ryan, R.E., Haeussler, H., Kayen, R.E., Hampton, M.A., Locat, J., Suleimani, E. and Alexander, C.R. (2007b) Reassessment of seismically induced tsunamigenic submarine slope failures in Port Valdez, Alaska, USA, *In*: Lycousis, V., Sakellarion, D., and Locat, J. (Eds.), Submarine Mass Movements and Their Consequences, 357-365.
Lee H.J., Ryan H.F., Kayen R.E., Haeussler P.J., Dartnell P., and Hampton M.A. (2006) Varieties of submarine failure morphologies of seismically-induced landslides in Alaskan fjords. *Nor. J. Geol.*, **86**, 221-230.
Lee, H.J., Schwab, W.C., Edwards, B.D., and Kayen, R.E. (1991) Quantitative controls on submarine slope failure morphology. *Mar. Geotech.*, **10**, 143-158.

Leroueil, S., Vaunat, J., Picarelli, L., Locat, J., Lee, H., and Faure, R. (1996) Geotechnical characterization of slope movements, *Proceedings of the International Symposium on Landslides*, Trondheim.

Locat, J., Gardner, J.V., Lee, H., Mayer, L., Hughes-Clarke, J.E., and Kammerer, E. (1999) Using multibeam surveys for submarine landslide investigations. *In*: Slope Stability Engineering, Yagi et al. Ed., Balkema, 127-134.

Locat, J., and Lee, H.J. (2002) Submarine landslides: advances and challenges. *Can. Geotech. J.*, **39**, 193-212.

Locat, J., Lee, H.J., Nelson, H.C., Schwab, W.C., and Twichell, D.C. (1996) Analysis of the mobility of far reaching debris flows on the Mississippi Fan, Gulf of Mexico. *7th Inter. Symp. on Landslides*, Senneset, ed., Balkema, 555-560.

Martin, R.G. and **Bouma, A.H.** (1982) Active diapirism and slope steepening, northern Gulf of Mexico continental slope. *Mar. Geotech.*, **5**, 63-91

McAdoo, B.G., Pratson, L.F., and Orange, D.L. (2000) Submarine landslide geomorphology, US continental slope, *Mar. Geol.,* **169**, 103-136.

Moore. J.G., Clague, D.A., Holcomb, R.T., Lipman, P.W., Normark, W.R., and **Torresan**, M.E. (1989) Prodigious submarine slides on the Hawaiian Ridge. *Jour. of Geophys. Res.*, **94**, 17,465-17,484.

Morgenstern, N.R. (1967) Submarine slumping and the initiation of turbidity currents. In: *Marine Geotechnique* (A.F. Richards, Ed.), University of Illinois Press, Urbana, Ill., p. 189-210.

Nelson, C.H. (1976) Late Pleistocene and Holocene depositional trends, processes, and history of Astoria Deep-Sea Fan, northeast Pacific. *Mar. Geol.*, **20**, 129-173.

Normark, W.R., Moore, J.G., and **Torresan, M.E.** (1993) Giant volcano-related landslides and the development of the Hawaiian Islands. In: *Submarine Landslides: Selected Studies in the U.S. EEZ* (Eds W.C. Schwab, H.J. Lee, and D.C. Twichell), *USGS Bull., **2002***, 184-196.

Orange, D.L. and **Breen, N.A.** (1992) The effects of fluid escape on accretionary wedges 2. seepage force, slope failure, headless submarine canyons, and vents. *J. of Geophys. Res.*, **97**, 9277-9295.

Parsons, T., Geist, E. L., Ryan, H. F., Lee, H. J., Haeussler, P. J., Lynett, P., Hart, P. E., Sliter, R. and Roland, E. (2014) Source and progression of a submarine landslide and tsunami: The 1964 Great Alaska earthquake at Valdez. *J. Geophys. Res. Solid Earth*, 119.

Piper, D.J.W., Cochonat, P, and Morrison, M.L. (1999) The sequence of events around the epicentre of the 1929 Grand Banks earthquake: initiation of debris flows and turbidity current inferred from sidescan sonar. *Sedimentology*, **46**, 79-97.

Plafker G., Kachadoorian R., Eckel E.B., Mayo, L.R. (1969) Effects of the earthquake of March 27, 1964 on various communities. US Geol. Surv. Prof. Pap. 542-G, 50.

Poulos, S.G., Castro, G., and France, J.W. (1985) Liquefaction evaluation procedure. *J. of Geotech. Eng.*, **111**, 772-791.

Prior, D.B., Bornhold, B.D., Coleman, J.M., and **Bryant, W.R.** (1982a) Morphology of a submarine slide, Kitimat Arm, British Columbia. *Geology*, **10**, 588-592.

Prior, D.B., Bornhold, B.D. and Johns, M.W. (1984) Depositional characteristics of a submarine debris flow. *J. of Geol.*, **92**, 707-727.

Prior, D.B., Bornhold, B.D., and **Johns, M.W.** (1986) Active sand transport along a

fjord-bottom channel, Bute Inlet, British Columbia. *Geology*, **14**, 581-584.

Prior, D.B. and **Coleman, J.M.** (1978) Disintegrating, retrogressive landslides on very low subaqueous slopes, Mississippi Delta. *Mar. Geotech.*, **3**, 37-60.

Prior, D.B., Coleman, J.M., and **Bornhold, B.D.** (1982b) Results of a known sea-floor instability event. *Geomar. Letters,* **2**, 117-122.

Prior, D.B., Wiseman, W.J., and **Gilbert, R.** (1981) Submarine slope processes on a fan delta, Howe Sound, British Columbia. *Geo-Mar. Letters*, **1**, 85-90.

Rabinovich, A.B., Thomson, R.E., Bornhold, B.D., Fine, I.V. and Kulikov, E.A. (2003) Numerical estimation of tsunami risk associated with landslide-generated tsunamis with application to the Strait of Georgia, British Columbia. *Pure and App. Geophy.*, **160**, 1273-1313.

Rabinovich, A. B, Thomson, R. E., Kulikov, E.A., Kulikov, Y.A., Bornhold, B.D., and **Fine, I.V.** (1999) The landslide-generated tsunami November 3, 1994, in Skagway. *Geophys. Res. Letters*, **26**, 3009-3012.

Robb, J.M. (1984) Spring sapping on the lower continental slope, offshore New Jersey. *Geology,* **12**, 278-282.

Ryan, H. F., Lee, H.J., Haeussler, P.J., Alexander, C.R., and Kayen, R.E., (2009) Historic and paleo-submarine landslide deposits imaged beneath port Valdez, Alaska; implications for tsunami generation in a glacial fjord, In. Mosher, D., Shipp, C, Moscardelli, l., Chaytor, J. D., Baxter, D., Lee, H. and Urgeles, R., (Eds.), Submarine Mass Movements and Their Consequences, 411-422.

Sangrey, D. (1977) Marine geotechnology—state of the art., *Mar. Geotech.*, **2**, 45-80.

Schwab, W.C. and **Lee, H.J.** (1983) Geotechnical analyses of submarine landslides in glacial marine sediment, northeast Gulf of Alaska. In: *Glacial Marine Sedimentation* (B.F. Molnia, Ed.), Plenum press, New York, p. 145-184.

Schwab, W.C., Lee, H.J., Twichell, D.C., Locat, J., Nelson, H.C., McArthur, M., and Kenyon, N.H. (1996) Sediment mass-flow processes on a depositional lobe, outer Mississippi Fan. *J. of Sed. Res.*, **66**, 916-927.

Seed, H.B. and **Rahman, M.S.** (1978) Wave-induced pore pressure in relation to ocean floor stability of cohesionless soils. *Mar. Geotech.*, **3**, 123-150.

Seed, H.B., Seed, R.B., Schlosser, F., Blondeau, F., and **Juran, I.** (1988) The landslide at the Port of Nice on October 16, 1979. *Earthquake Engineering Research Center (University of California, Berkeley),* **Report No. UCB/EERC-88/10**, 68 pp.

Silva, A.J., Baxter, C.D.P., LaRosa, P.T., and **Bryant, W.R.** (2004) Investigation of mass wasting on the continental slope and rise. *Mar. Geol.*, **203**, 355-366.

Sultan, N., Cochonat, P., Foucher, J.P., Mienert, J., Haflidason, H., and **Sejrup, H.P.**, (2003) Effect of gas hydrates dissociation on seafloor slope stability, In: *Submarine Mass Movements and their Consequences*,*1st Inter. Symp.* (J. Locat and J. Mienert, Eds.), p. 103-111.

Syvitski, J.P.M., Burrell, D.C., and **Skei, J.M**. (1987) *Fjords: Processes and Products.* Springer-Verlag, New York, 379 pp.

Tappin, D.R., Watts, P. and **Matsumoto, T.**, (2003) Architecture and failure mechanism of the offshore slump responsible for the 1998 Papua New Guinea Tsunami. In: *Submarine Mass Movements and their Consequences, 1st Inter. Symp.* (J. Locat, and J. Mienert, Eds.), p. 383-389.

Terzaghi, K. (1956) Varieties of submarine slope failures. *Proc. 8th Tex. Conf. of Soil*

Mech. and Found. Eng., Bureau Eng. Research, Tex. Univ., Spec. Publ., **29**, 1-41.
Van Kessel, T. and Kranenburg, C. (1998) Wave-induced liquefaction and flow of subaqueous mud layers. *Coastal Engineering*, **34**, 109-127.

Fig. 1. Oblique view of multibeam imagery in the Santa Barbara Channel, southern California (after Eichhubl et al. 2002). The Figure shows a large landslide complex near the center (Goleta Slide, about 10 km x 10 km) and a smaller landslide near the left margin (Gaviota mudflow, 2 km x 2 km). The space between the failures has not failed. Properties of a sediment core in the stable area were obtained on Piston Core 601-P1.

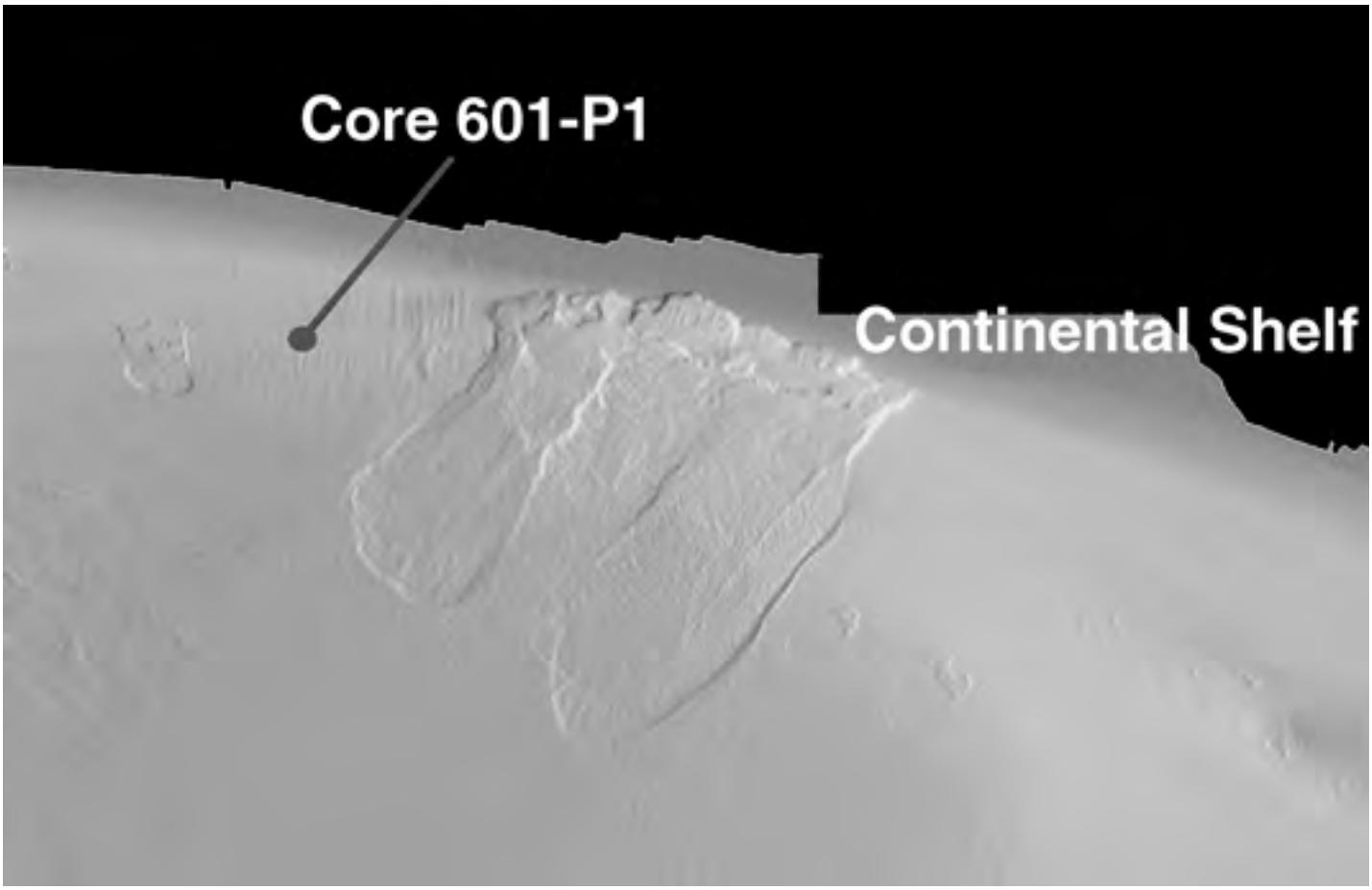

Fig. 2. Multibeam imagery of the continental margin off Los Angeles California showing a slope dominated by landslide activity on a steep slope (15-20°) and other more gentle slopes to the northwest that do not show indications of failure (after Lee et al. 2000).

Fig. 3. Shear strength of Piston Core 601 P1 compared with an estimated normally consolidated strength profile (Lee, et al., 2004).

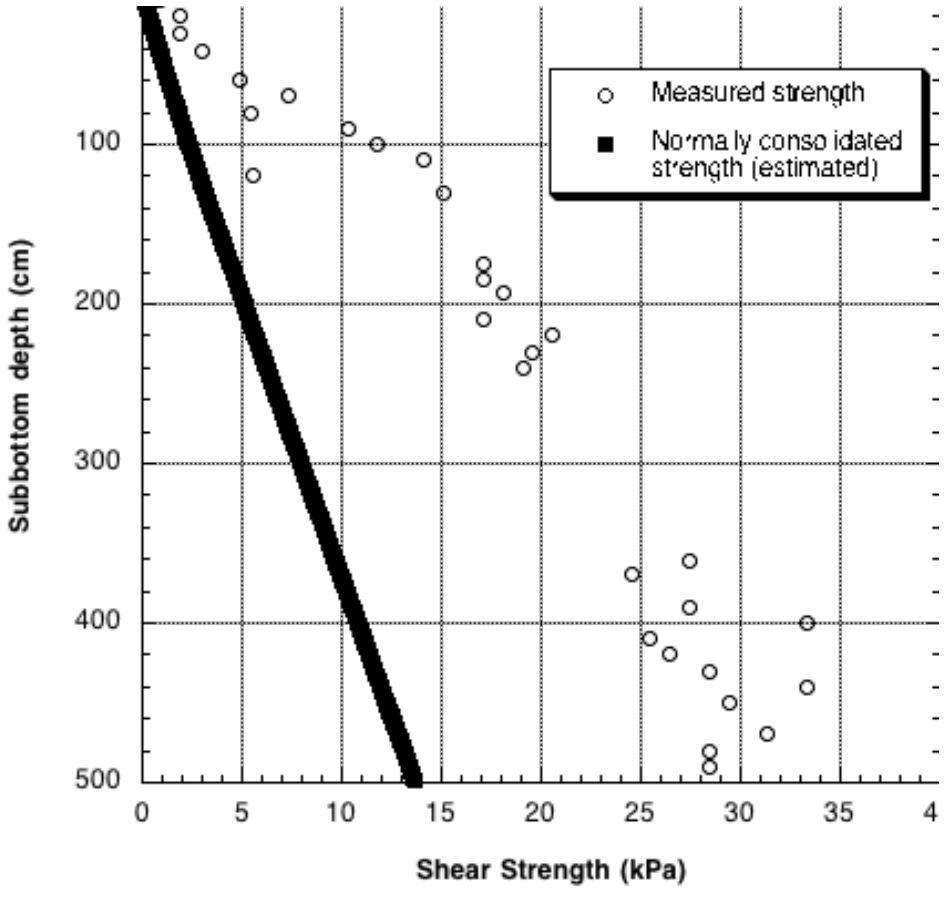

Fig. 4. Void ratio-effective stress data showing the response of sediment to four bursts of cyclic loading (simulated “earthquakes”)(Lee et al., 2004).

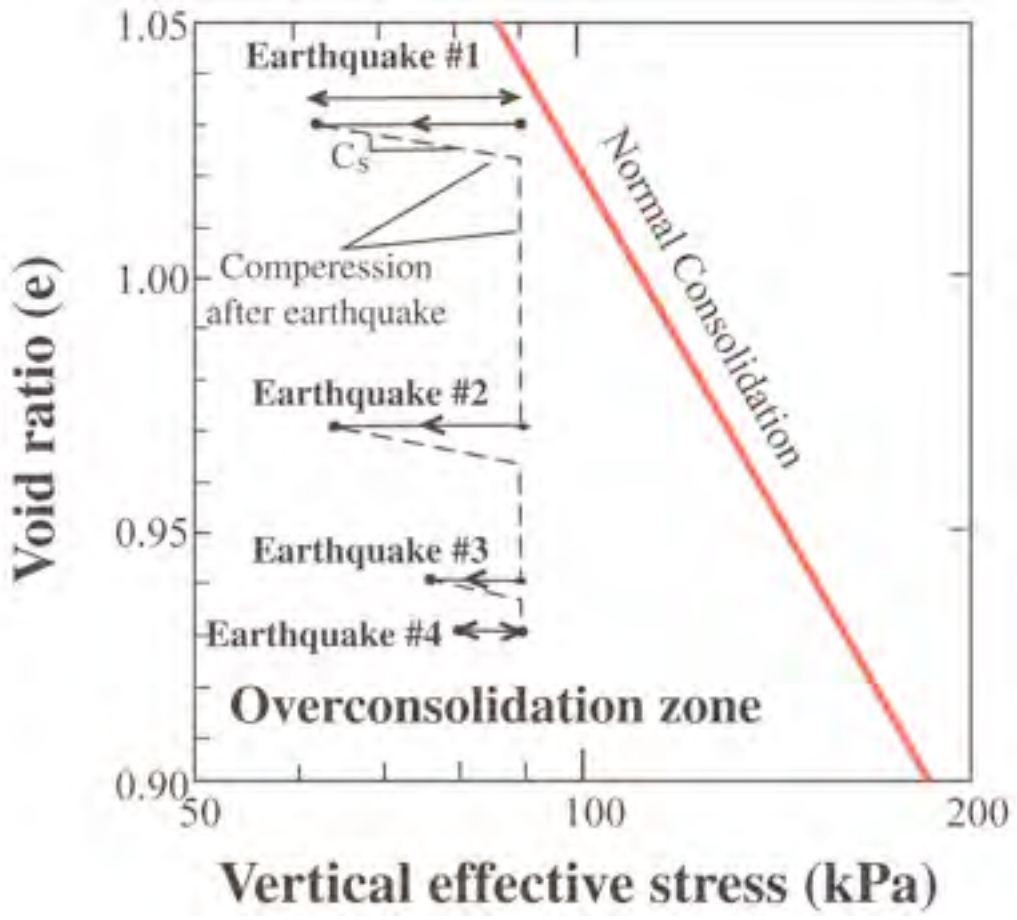

Fig. 5. Steady state of deformation line (after Lee *et al*. 1991). If the initial sediment state lies above the steady state line, there will be a tendency toward the generation of positive pore pressures during a failure event (e.g., an earthquake). Such pore pressure generation will lead to a dramatic decrease in shear strength and will increase the tendency for sediment flows. An initial sediment state below the steady state line will produce dilatant behavior, negative pore pressure generation, and decreased tendency to flow.

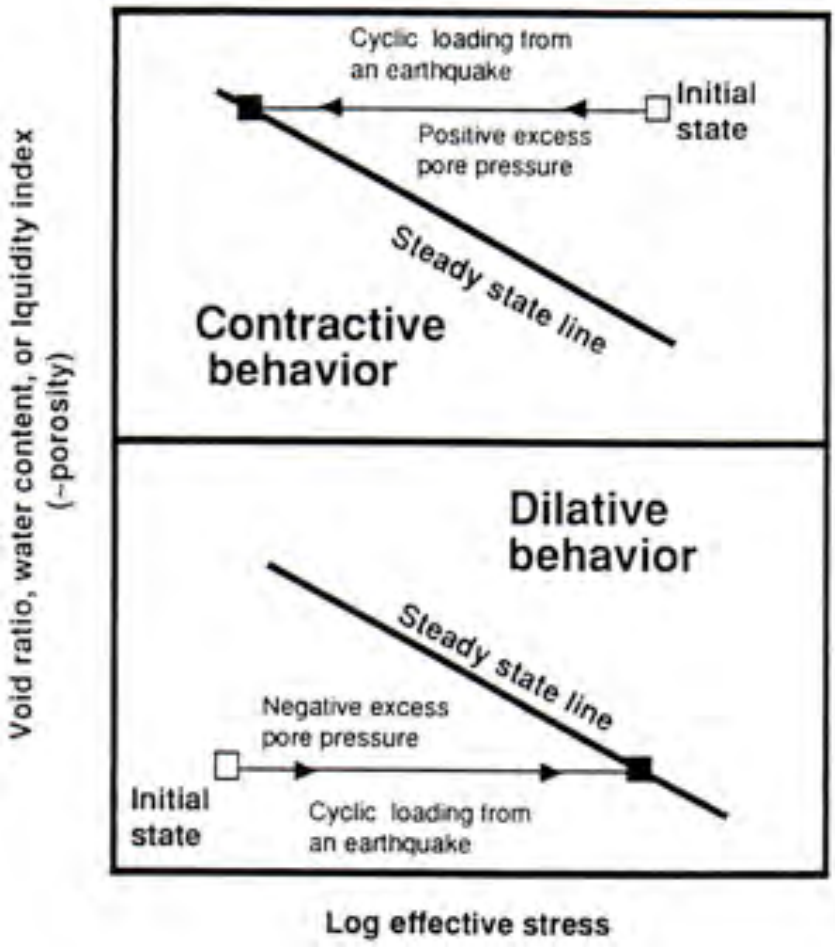

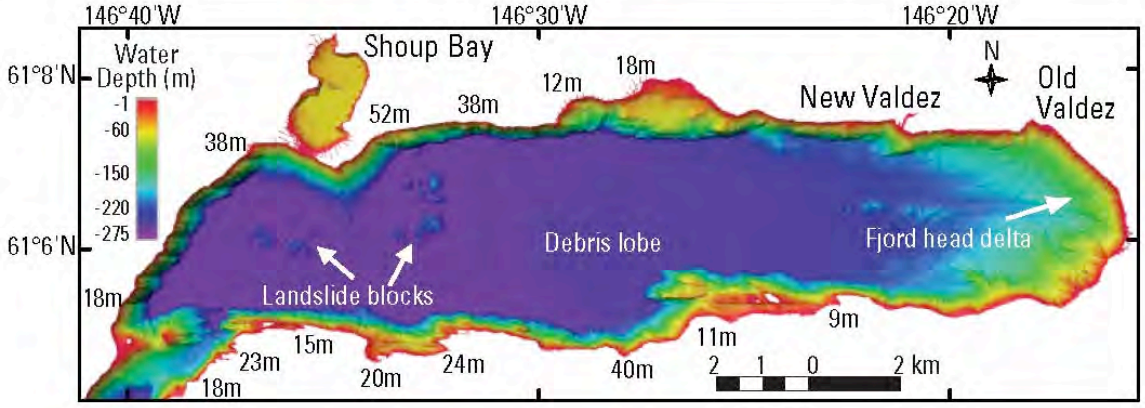

Figure 6. Multibeam imagery of Port Valdez showing landslide features discussed in the text (Lee et al., 2007b). Labels around margin of the fjord show the estimated tsunami wave heights (runups) resulting from the 1964 earthquake (Plafker et al., 1969).

Figure 7. Map showing changes in bathymetric depth between surveys run in 1901 and 1966, spanning the 1964 earthquake (Lee et al., 2007b).

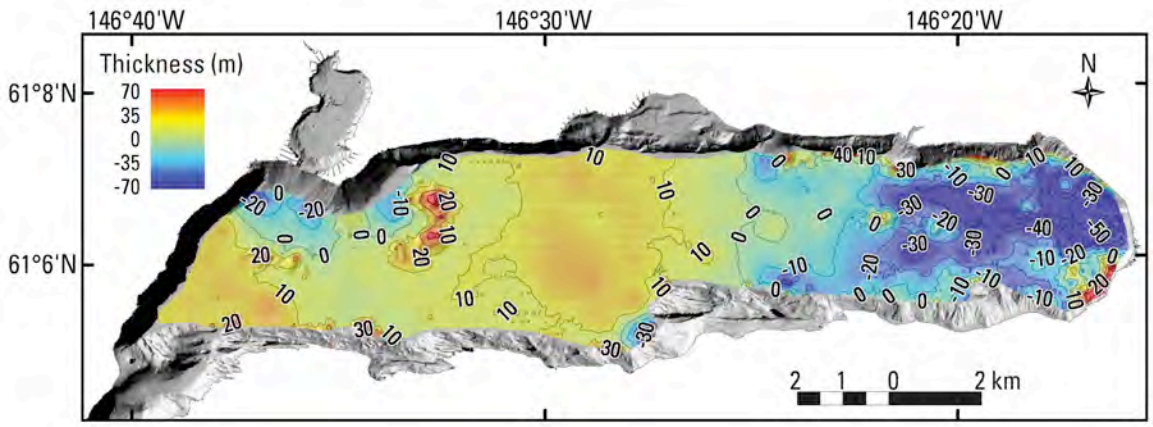

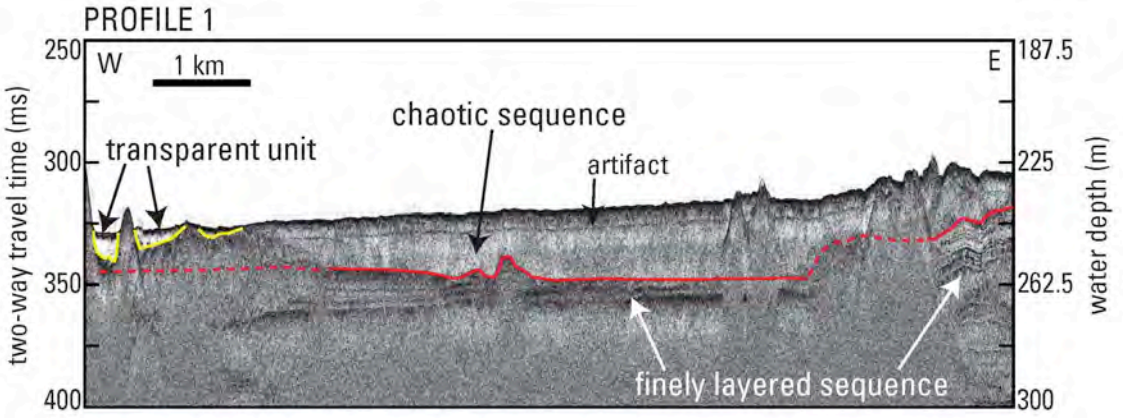

Figure 8. E-W chirp profile line across northern part of Port Valdez (Lee et al., 2007b). Acoustic facies features discussed in text are identified.